RSC Advances

ROYAL SOCIETY OF CHEMISTRY

www.rsc.org/advances

Cite this: DOI: 10.1039/c0xx00000x

www.rsc.org/xxxxxx

ARTICLE TYPE

Role of SDS surfactant concentrations on the structural, morphological, dielectric and magnetic properties of $CoFe_2O_4$ nanoparticles

M. Vadivel[a], R. Ramesh Babu[a,*], M. Arivanandhan[b], K. Ramamurthi[c], Y. Hayakawa[b]

Received (in XXX, XXX) Xth XXXXXXXXX 20XX, Accepted Xth XXXXXXXXX 20XX

DOI: 10.1039/b000000x

Abstract

In this work, we report on the preparation of sodium dodecyl sulfate (SDS) surfactant added cobalt ferrite ($CoFe_2O_4$) magnetic nanoparticles by co-precipitation method for various concentrations (0.04, 0.08, 0.12, 0.16 and 0.20 M) of SDS. The formation of single phase cubic spinel structure is confirmed by XRD analysis. FTIR study confirms the presence of Fe-O symmetrical stretching vibration in tetrahedral site. TEM images imply that the SDS surfactant significantly limits the agglomeration of $CoFe_2O_4$ nanoparticles. Dielectric study reveals that the SDS added $CoFe_2O_4$ has high dielectric constant than that of pure $CoFe_2O_4$ nanoparticles. Magnetic measurement showed the enhanced saturation magnetization (138.75 emu/g), coercivity (775.69 O_e) and retentivity (60.23 emu/g) for 0.08 M SDS added $CoFe_2O_4$ nanoparticles. Further, the results obtained in the present study suggest that the surfactant can significantly modify the size and morphology of the prepared $CoFe_2O_4$ nanoparticles.

Introduction

Nowadays, considerable efforts have been taken on the nanoscale ferrite magnetic materials due to their extraordinary electrical, optical, thermal, mechanical and magnetic properties when compared with that of their corresponding bulk counterparts.[1] Hence, several types of ferrite magnetic nanoparticles have been investigated for various applications. Especially, spinel ferrite magnetic nanoparticles are of great interest due to their applications in magnetic storage devices, microwave devices, lithium ion batteries, drug delivery, magnetic resonance imaging (as a contrast agent) and ferrofluids.[1-4] Spinel ferrites have the general molecular formula, AB_2O_4 (where A and B are divalent and trivalent metal cations, respectively). Among the spinel ferrites, cobalt ferrite ($CoFe_2O_4$) belongs to the face centered cubic inverse spinel structure in which two types of sites are always present such as tetrahedral (A) site and octahedral (B) site.[5] $CoFe_2O_4$ magnetic nanoparticles have received much attention due to their outstanding properties such as high magnetocrystalline anisotropy, high magnetostriction, moderate saturation magnetization (80 emu/g), high coercivity (5400 Oe) at room temperature, high electrical resistivity, excellent thermal stability and high mechanical hardness.[5] It is well established that the size, morphology, purity and distribution of particles are the key parameters in determining the properties of magnetic materials at nanoscale level.[6] Synthesis methods also play an important role in controlling the key parameters to make them for potential applications. In recent years, numerous chemical methods have been employed in the preparation of pure $CoFe_2O_4$ as well as substituted $CoFe_2O_4$ nanoparticles which include the auto-combustion,[1] citrate gel,[5] co-precipitation,[7] sol-gel,[8] hydrothermal[9] and surfactant-assisted[10] methods. Among these, chemical co-precipitation is one of the inexpensive methods for the preparation of well dispersed uniform size particles with smaller time duration and less reaction temperature.[7] It is also possible to achieve the desired size and shape of the particles from co-precipitation method by controlling the various key parameters such as reaction temperature, stirring speed and pH of the reactants.[7] Nucleation and growth rates are also the important factors to control the size and morphology of the particles since they strongly affect the precipitation conditions. Maaz et al.[11] showed that there is a possibility to obtain relatively smaller particles from co-precipitation method if the nucleation rate is higher than that of the growth rate.

Surface active agent (surfactant) also plays a vital role to control the size of the nanoparticles due to its electrostatic repulsion and steric hindrance properties.[12,13] Further, magnetic nanoparticles have strong tendency to agglomerate due to interparticle magnetic interaction and large nanoparticles surface reactivity. In order to prevent agglomeration and oxidation from the atmospheric oxygen, the magnetic nanoparticles are usually coated with some surfactant.[11] Therefore, the choice of appropriate surfactant is important to tailor the size and morphology of the magnetic

***Corresponding Author:** E-mail : rampap2k@yahoo.co.in*
Tel : +91-431-2407057, Fax : +91-431-2407045
[a]Crystal Growth and Thin Film Laboratory, Department of Physics, Bharathidasan University, Tiruchirappalli 620024, Tamil Nadu, India.
[b]Nanomaterials Laboratory, Research Institute of Electronics, Shizuoka University, Hamamatsu 4328011, Japan.
[c]Crystal Growth and Thin Film Laboratory, Department of Physics and Nanotechnology, Faculty of Engineering and Technology, SRM University, Kattankulathur 603203, Tamil Nadu, India.

nanoparticles in the co-precipitation method. Recently, the influence of surfactant on the properties of nanoparticles prepared by various methods are reported.[2,3,6,7,13-20] Zhao et al.[13] reported on the enhanced magnetic properties of sodium dodecyl sulfate surfactant coated $ZnLa_{0.02}Fe_{1.98}O_4$ nanoparticles prepared using solvothermal method. Shen et al.[16] investigated and reported the facile co-precipitation synthesis of shape controlled magnetite (Fe_3O_4) nanoparticles by varying the amount of sodium dodecyl sulfate. To the best of our knowledge, no reports are available on the effect of properties of $CoFe_2O_4$ nanoparticles due to adding various concentrations of sodium dodecyl sulfate (SDS) in the synthesis. Hence, in the present work, the role of various concentrations of SDS in the preparation of $CoFe_2O_4$ nanoparticles by co-precipitation method and their structural, morphological, dielectric and magnetic properties are reported.

Experimental section

Materials and methods

Iron (III) chloride hexahydrate ($FeCl_3.6H_2O$, Merck, 99%), cobalt (II) chloride hexahydrate ($CoCl_2.6H_2O$, Merck, 98%), sodium dodecyl sulfate (SDS, Sigma Aldrich, 99%) and sodium hydroxide (NaOH, Merck, 97%) were used as the starting materials. SDS and NaOH were used as surface active agent and precipitation agent, respectively. Double distilled water was used as solvent for the preparation of $CoFe_2O_4$ and various concentrations of SDS added $CoFe_2O_4$ nanoparticles. All chemicals were used as received without further purification.

Synthesis of SDS added $CoFe_2O_4$ nanoparticles

Co-precipitation method was adopted for preparation of $CoFe_2O_4$ and various concentrations of SDS added $CoFe_2O_4$ nanoparticles. The experimental procedure for the synthesis of pure $CoFe_2O_4$ nanoparticles by the co-precipitation method is discussed elsewhere.[21] For the preparation of SDS added $CoFe_2O_4$ nanoparticles, 0.4 M iron (III) chloride hexahydrate, 0.2 M cobalt (II) chloride hexahydrate and SDS were dissolved separately in 25 ml of double distilled water at room temperature. Subsequently, the prepared chloride precursor solutions were mixed well together and then the various levels of SDS solution (0.04, 0.08, 0.12, 0.16 and 0.20 M) were added during the reaction to avoid the formation of agglomeration in solution. The whole mixture was stirred vigorously at room temperature for 30 minutes to obtain homogeneous solution. 3 M NaOH aqua solutions prepared from NaOH pellets was then added into the prepared solution by dropwise which resulted in the precipitation of the $CoFe_2O_4$ nanoparticles. In this work a pH of 13 was set to obtain the high yield of the product. The net solution mixture was vigorously stirred at 80 °C for 3 h. After completion of the precipitation process, the final product was allowed to cool down to room temperature naturally. The black color precipitate was collected at the bottom of the flask and the precipitated particles were washed several times using double distilled water followed by ethanol. After that the prepared black color precipitate was dried at 50 °C for 24 h and then annealed at 600 °C for 3 h to improve the crystallinity.

Characterization

Rigaku X-ray diffractometer was used to confirm the crystalline nature and crystal system of $CoFe_2O_4$ and SDS added $CoFe_2O_4$ nanoparticles. The presence of functional groups was confirmed by recording Fourier transform infrared (FTIR) spectrum in the range of 4000-400 cm^{-1} using JASCO 460 plus FTIR spectrometer. Size and morphology of the particles were determined using transmission electron microscopic (TEM) (Microscope JEM-2100F) analysis. Magnetic properties were studied at room temperature using a Lakeshore-7404 vibrating sample magnetometer (VSM) technique. Dielectric measurements were carried out as a function of frequency (100 Hz - 1MHz) and temperature (room temperature to 100 °C) using HIOKI 3532-50 LCR HiTESTER. For this measurement, 1 mm thick and 13 mm diameter pellets were prepared using the manual hydraulic press machine and then high grade silver paste was applied on both sides of pellets for better contact with the electrode. The real part of the dielectric constant (ε') was calculated using the relation $\varepsilon' = Cd/(\varepsilon_0 A)$, where C is the capacitance of the pellet in farad, d is the thickness of the pellet in meter, A is the cross sectional area of the pellet in square meter, and ε_0 is the dielectric permittivity of free space (8.854×10^{-12} F/m). The imaginary part of the dielectric loss (ε'') was determined using the relation $\varepsilon'' = \varepsilon' D$, where D is the dissipation factor.

Results and discussion

X-ray diffraction analysis

XRD patterns of the prepared $CoFe_2O_4$ and various concentrations of SDS (SDS: 0.04, 0.08, 0.12, 0.16 and 0.20 M) surfactant added $CoFe_2O_4$ nanoparticles are shown in Fig. 1a. The XRD peaks of $CoFe_2O_4$ nanoparticles perfectly match with JCPDS data (card no.: 22-1086). Further, the presence of (hkl) planes such as (111), (220), (311), (400), (422), (511), (440) and (533) indicates the formation of a single phase cubic inverse spinel structure of $CoFe_2O_4$ with Fd3m space group. The sharp and strong peaks reveal the high crystallinity of the synthesized nanoparticles. Moreover, the high intense (311) diffracted peak position is slightly shifted towards the lower angle side by increasing the SDS concentrations in $CoFe_2O_4$ nanoparticles and its variation is shown in Fig. 1b. Further the intensity of (311) peak increases with increasing SDS concentration up to 0.16 M then it decreases for higher concentrations of SDS. The average crystallite size was calculated from (311) diffracted peak using Debye-Scherrer's formula[22] $t = k\lambda/(\beta\cos\theta)$, where the constant k depends upon the structure of the crystallite (present case, k = 0.9), λ is the wavelength of X-rays used (CuKα: 1.5405Å), β is the fullwidth at halfmaximum of diffraction peak (311) and θ is the angle of diffraction. The calculated average crystallite size values are presented in Table 1. From the table, it can be observed that the average crystallite size of $CoFe_2O_4$ nanoparticles increases from 15 nm to 24 nm, due to addition of surfactant concentration up to 0.08 M. Further increasing SDS concentration from 0.12 to 0.20 M the average crystallite size decreases to 15 nm. The lattice constant *a* was calculated for (311) peak using the relation $a = d\sqrt{h^2+k^2+l^2}$ and is listed in Table 1, where d is the interplanar distance and (hkl) are the Miller indices. Further, it is observed that the lattice constant and

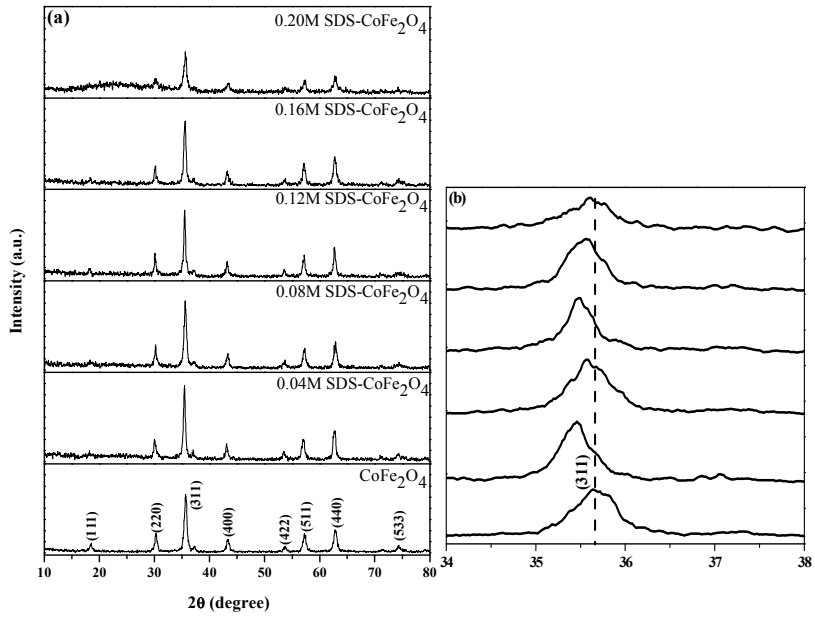

Fig. 1 (a) XRD patterns of $CoFe_2O_4$ and various concentrations of SDS added $CoFe_2O_4$ nanoparticles (b) variation in (311) diffracted peak position

Table 1 Average crystallite size (t_{311}), lattice constant (a), unit volume cell (V_{cell}), hopping length for tetrahedral site (L_A), hopping length for octahedral site (L_B), Fe-O vibrations (wavenumber-ν), particle size (l), saturation magnetization (M_s), coercivity (H_c) and retentivity (M_r) of $CoFe_2O_4$ and various concentrations of SDS added $CoFe_2O_4$ nanoparticles

Sample	XRD					FTIR	TEM	VSM		
	Average crystallite size (t_{311}) (nm)	Lattice constant (a) (Å)	Volume (V_{cell}) (Å)	L_A (nm)	L_B (nm)	Fe-O vibration (wavenumber-ν) (cm^{-1})	Particle size (l) (nm)	M_s (emu/g)	H_c (O_e)	M_r (emu/g)
$CoFe_2O_4$	15.57	8.3811	588.71	3.6290	2.9627	587	16.4	61.45	681.04	20.02
0.04 M SDS-$CoFe_2O_4$	20.38	8.3811	588.71	3.6290	2.9627	590	15.7	137.72	552.30	41.46
0.08 M SDS-$CoFe_2O_4$	24.31	8.3844	589.40	3.6304	2.9638	588	--	138.75	775.69	60.23
0.12 M SDS-$CoFe_2O_4$	19.25	8.3890	590.37	3.6324	2.9655	589	27.1	62.68	581.65	22.04
0.16 M SDS-$CoFe_2O_4$	15.65	8.3615	584.59	3.6205	2.9557	588	--	62.22	691.42	24.14
0.20 M SDS-$CoFe_2O_4$	15.56	8.3661	585.55	3.6225	2.9574	588	13.9	53.26	585.10	20.24

unit cell volume of surfactant added $CoFe_2O_4$ nanoparticles initially increase and then decrease when compared with that of $CoFe_2O_4$ nanoparticles. Hopping length for tetrahedral site (L_A) and octahedral site (L_B) was calculated using the following relation,[23] $L_A = a\sqrt{3}/4$ and $L_B = a\sqrt{2}/4$ and is given in Table 1. From the result, it is concluded that the hopping length of L_A and L_B varies directly with lattice constant.

FTIR spectral analysis

FTIR spectroscopy is a very useful technique to deduce the structural investigation and to identify the distribution of cations between tetrahedral and octahedral sites of the inverse spinel structure of $CoFe_2O_4$ nanoparticles. The recorded FTIR spectra of $CoFe_2O_4$ and the SDS added $CoFe_2O_4$ nanoparticles are shown in Fig. 2. Two main broad metal-oxygen bands are observed in all spinel ferrite system which corresponds to intrinsic stretching vibrations of the metal at tetrahedral site (ν_1) (600-500 cm^{-1}) and octahedral site (ν_2) (430-385 cm^{-1}).[24] Generally, more energy is required for the Fe-O stretching vibration occupying the tetrahedral site than the corresponding octahedral site since the bond length of tetrahedral lattice site is much shorter than that of octahedral site.[25] In the present case, a strong band observed at 587 cm^{-1} is assigned to the symmetrical stretching vibration of Fe-O (metal-oxygen) at tetrahedral site. The absorption bands observed at 1629 and 3429 cm^{-1} suggest that the presence of symmetric H-O-H bending and O-H stretching vibrations, respectively. Further, it can be concluded that there is no observable shift in Fe-O symmetrical stretching vibration at

tetrahedral site due to the addition of SDS in $CoFe_2O_4$ nanoparticles, thus indicating the SDS molecule does not affect the structural characteristics of $CoFe_2O_4$ nanoparticles.

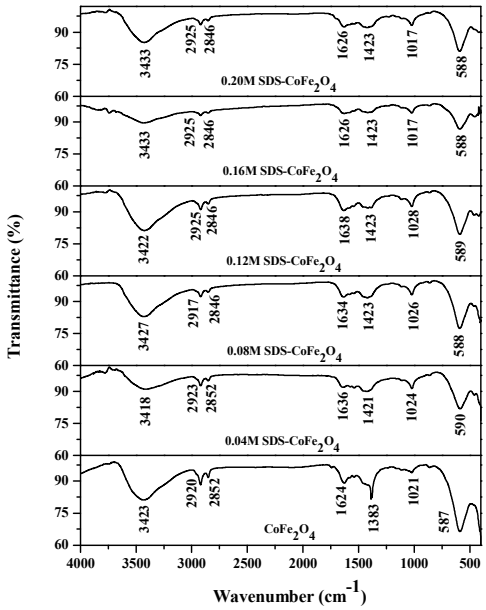

Fig. 2 FTIR spectra of $CoFe_2O_4$ and various concentrations of SDS added $CoFe_2O_4$ nanoparticles

TEM and HRTEM measurements

Effect of the surfactant concentrations on the size and morphology of the $CoFe_2O_4$ nanoparticles is studied by TEM measurement. Figs. 3a-d show the TEM micrographs of $CoFe_2O_4$, 0.04 M SDS-$CoFe_2O_4$, 0.12 M SDS-$CoFe_2O_4$ and 0.20 M SDS-$CoFe_2O_4$ nanoparticles respectively. From these figures, it is clearly seen that the size and morphology of the prepared nanoparticles are remarkably modified by increasing the SDS concentration in $CoFe_2O_4$ nanoparticles. Generally, the size of the nanoparticles can be controlled by controlling the interparticle interaction (particle-particle interaction) between the magnetic nanoparticles due to the addition of surfactants.[13] The change in morphology from irregular to regular shape indicates that the nucleation and growth of the particles are affected by the addition of SDS.[26] Also, from the TEM images, the average particle size *(l)* of $CoFe_2O_4$ and 0.04 M, 0.12 M, 0.20 M SDS added $CoFe_2O_4$ nanoparticles is calculated and their corresponding histogram images are shown in Figs. 4a-d. The results reveal that the particle size initially increases and then decreases with increasing SDS concentrations. Moreover, the particle size obtained from TEM analysis is slightly larger than that of the calculated from XRD analysis and the calculated values are presented in Table 1. Due to the steric hindrance and stabilization properties of surfactants one can expect the reduction in size of the ferrite magnetic nanoparticles.[13] But, in the present work, we have

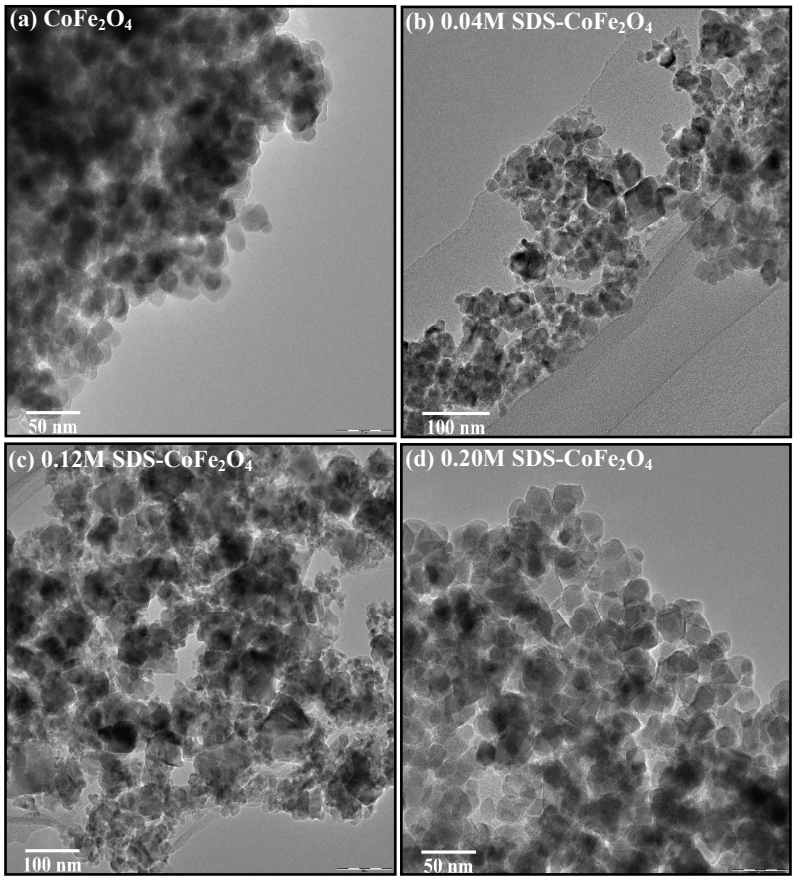

Fig. 3 TEM images of (a) $CoFe_2O_4$ and (b) 0.04 M (c) 0.12 M (d) 0.20 M SDS added $CoFe_2O_4$ nanoparticles

obtained the larger size particles for 0.12 M concentration of SDS added $CoFe_2O_4$ nanoparticles compared with that of pure and 0.04 M concentration of SDS added $CoFe_2O_4$ nanoparticles. The increase in particle size at lower concentration (from 0.04 to 0.12 M) may be due to the reason that the concentration of SDS surfactant molecules is not enough to control the interparticle interaction which leads to agglomeration between the particles. However, further increase in the surfactant concentration (from 0.12 to 0.20 M) controls the particle interaction between the magnetic nanoparticles and hence the agglomeration gets reduced. HRTEM images of some selected concentrations are shown in Figs. 5a-d and the clear lattice boundary in HRTEM images illustrates the high crystallinity of the prepared $CoFe_2O_4$ and SDS added $CoFe_2O_4$ nanoparticles. From HRTEM analysis, the crystal lattice spacings determined are 0.251, 0.198, 0.489 and 0.476 nm for $CoFe_2O_4$, 0.04 M SDS-$CoFe_2O_4$, 0.12 M SDS-$CoFe_2O_4$ and 0.20 M SDS-$CoFe_2O_4$ nanoparticles, respectively which corresponds to (311), (331), (111) and (111) lattice plane of $CoFe_2O_4$ nanoparticles. These results agree well with the standard JCPDS data (card no.: 22-1086).

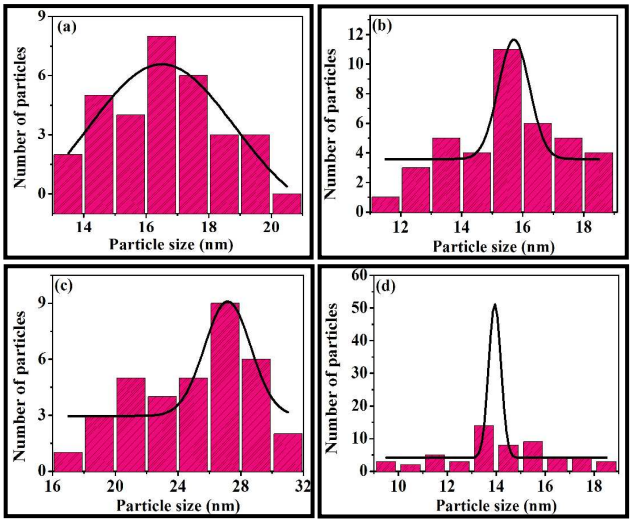

Fig. 4 Histogram images of (a) $CoFe_2O_4$ and (b) 0.04 M (c) 0.12 M (d) 0.20 M SDS added $CoFe_2O_4$ nanoparticles

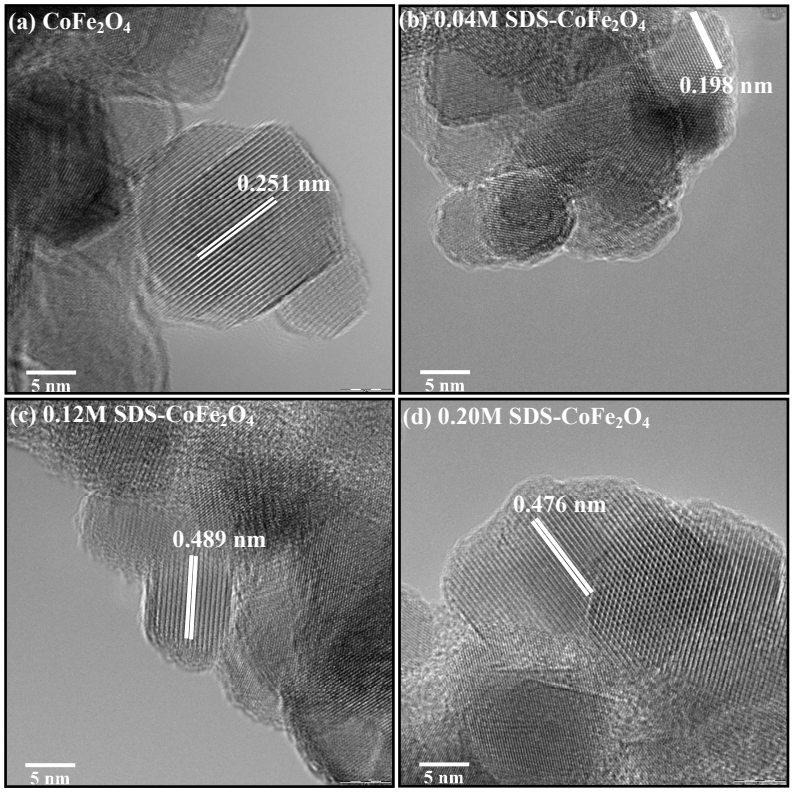

Fig. 5 HRTEM images of (a) $CoFe_2O_4$ and (b) 0.04 M (c) 0.12 M (d) 0.20 M SDS added $CoFe_2O_4$ nanoparticles

Dielectric properties

Figs. 6a and 6b show the dielectric constant and dielectric loss of $CoFe_2O_4$ and various concentrations of SDS added $CoFe_2O_4$ nanoparticles as a function of frequency at room temperature. It can be seen from the figures that both the dielectric constant and dielectric loss factors decrease with increasing frequency and have become almost constant in the higher frequency region for all surfactant concentrations. The variation in dielectric constant with frequency at different temperatures of all the prepared $CoFe_2O_4$ nanoparticles is shown in Figs. 7a-f. From these figures, it is observed that the dielectric constant is very high at lower frequency region and decreases with increasing frequency for all temperatures. The decrease in dielectric constant with increasing frequency is a normal dielectric behavior of ferrite magnetic nanomaterials. Such kind of behaviour can be explained on the basis of Maxwell-Wagner and Koops phenomenological theory.[1,5] According to this model, in ferrites, the dielectric structure is assumed to consist of well conducting grains which are separated by the poorly conducting grain boundaries.[27] The grains are strongly effective at higher frequencies and the grain boundaries are dominant at lower frequencies. This causes the localized accumulation of charge carriers under the applied electric field and thereby enhancing the space charge polarization thus the dielectric constant is enhanced at lower frequency region. As the frequency of the applied field continues to increase, the electrons cannot keep up with the applied field and the alteration of their direction lags behind that of the field. This decreases the probability of electrons reaching the grain boundary and as a result the polarization decreases. Therefore, the dielectric constant decreases with increasing applied electric field.[6] The dielectric constant and dielectric loss of SDS added $CoFe_2O_4$ is relatively high when compared with that of pure $CoFe_2O_4$ nanoparticles which indicates that the surfactant improves the dielectric properties and the prepared samples may be useful for high frequency applications.

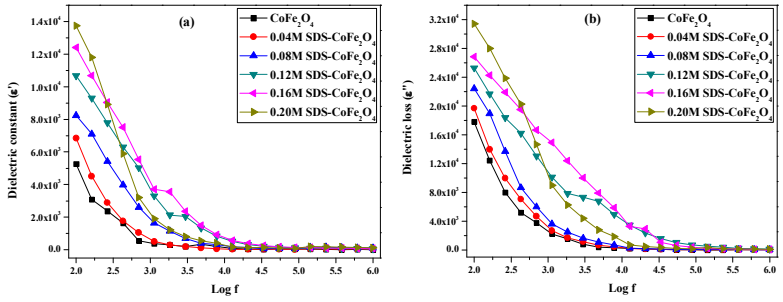

Fig. 6 (a) Variation of dielectric constant (ε') and (b) dielectric loss (ε'') as a function of frequency for $CoFe_2O_4$ and various SDS added $CoFe_2O_4$ nanoparticles

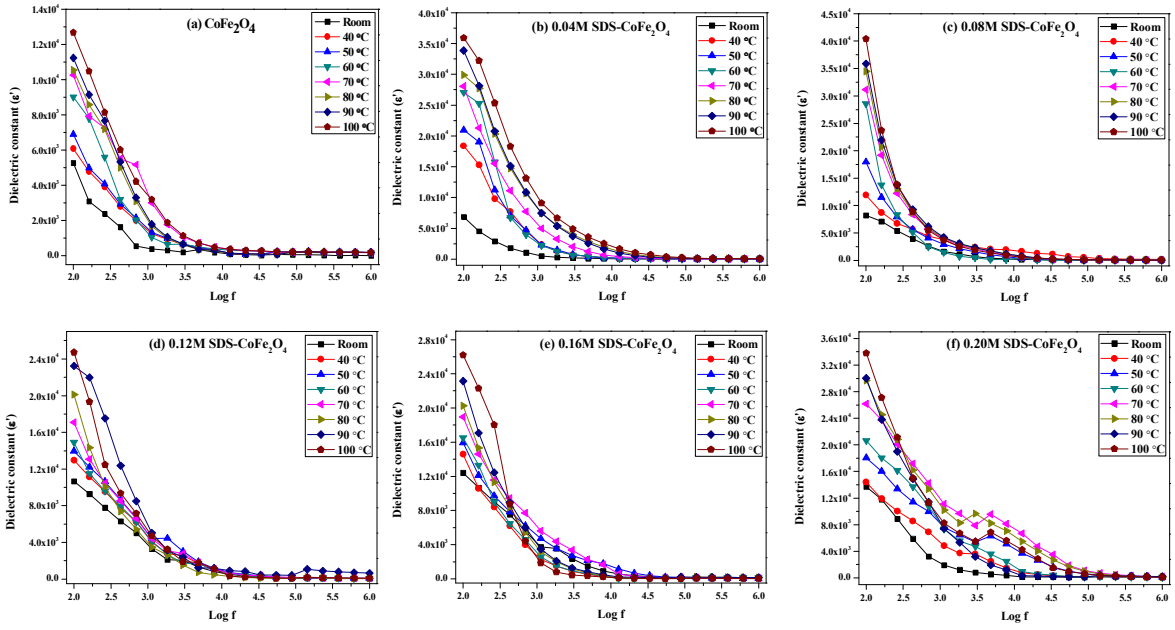

Fig. 7 Variation of dielectric constant (ε') at different temperatures for $CoFe_2O_4$ and various SDS added $CoFe_2O_4$ nanoparticles as a function of frequency

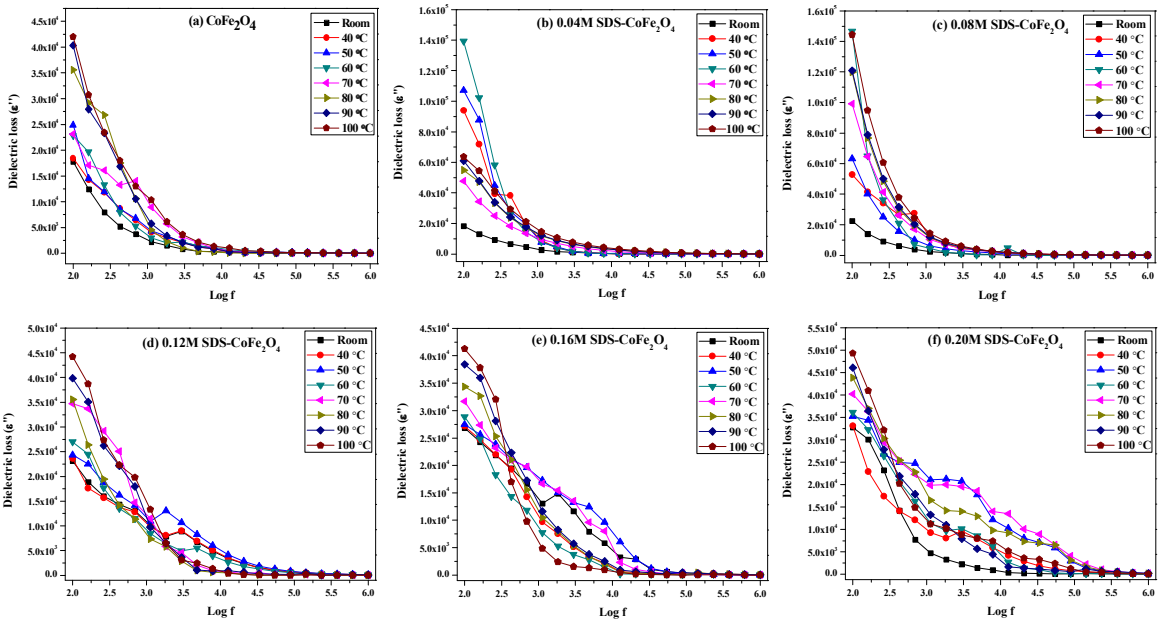

Fig. 8 Variation of dielectric loss (ε") at different temperatures for $CoFe_2O_4$ and various SDS added $CoFe_2O_4$ nanoparticles as a function of frequency

From the Figs. 7a-f, it is also observed that the dielectric constant initially increases slowly with temperature and then increases rapidly with increasing temperature for pure as well as various concentrations of SDS added $CoFe_2O_4$ nanoparticles. This type of behaviour at higher temperature may be due to generation of extra thermal energy which enhances the mobility of charge carriers. This increases the polarization and hence the dielectric constant increases. But, at low temperatures, the thermal energy is not sufficient to contribute to the mobility of charge carriers and hence low dielectric constant.[28] Figs. 8a-f show the variation in dielectric loss as a function of frequency for various temperatures which also exhibit the similar trend in dielectric constant.

Vibrating sample magnetometer analysis

Fig. 9 shows the room temperature magnetic hysteresis loop of $CoFe_2O_4$ and various concentrations of the SDS added $CoFe_2O_4$ nanoparticles. The magnetic parameters such as saturation magnetization (M_s), coercivity (H_c) and retentivity (M_r) are extracted from the magnetization curve which reveals that all the prepared nanoparticles show a ferromagnetic nature at room temperature and the values observed are presented in Table 1. From the results, it can be noticed that the value of M_s is high for 0.04 and 0.08 M of SDS added $CoFe_2O_4$ nanoparticles than that of pure $CoFe_2O_4$ nanoparticles. Thus the increase in M_s value for 0.04 and 0.08 M SDS concentrations may be due to the increase in particle size and crystallinity.[13] Further, the M_s value gradually decreases with increasing SDS concentration (0.12-0.20 M) in $CoFe_2O_4$ nanoparticles which may be attributed to the large surface-to-volume ratio. Also, the smaller particle size leads to the structural disorder on the surface of the nanoparticles and thereby reduces the saturation magnetization as has also been observed by Shen et al.[16] Zhao et al.[13] reported a maximum value of M_s (101.0 ± 0.2 emu/g) for SDS added $ZnLa_{0.02}Fe_{1.98}O_4$ cluster prepared by solvothermal method. Shen et al.[16] reported a maximum M_s value for nanocubes (108.1 emu/g) when compared with that of nanospheres (75.9 emu/g) and nanoneedles (94.2 emu/g) in magnetite (Fe_3O_4) system obtained by facile co-precipitation method. In the present work, the maximum M_s values obtained is 137.72 emu/g and 138.75 emu/g respectively for 0.04 M and 0.08 M of SDS added $CoFe_2O_4$ nanoparticles. Further, 0.08 M of SDS added $CoFe_2O_4$ nanoparticles show the maximum H_c and M_r values. But for higher SDS concentrations (0.12-0.20 M) the H_c and M_r value decreases. Thus the present results conclude that the decrease in H_c and M_r values at higher SDS concentrations may be attributed to the reduction in size of the particles since the surface disorder is high when the surface to volume ratio is large.[15]

Conclusion

In summary, $CoFe_2O_4$ and various concentrations of SDS surfactant added $CoFe_2O_4$ nanoparticles were successfully prepared by co-precipitation method. XRD analysis confirms the single phase cubic inverse spinel structure of the prepared nanoparticles. The average crystallite size of $CoFe_2O_4$ nanoparticles initially increases thereafter decreases with increasing SDS concentration. The formation of Fe-O symmetrical stretching vibration in tetrahedral site was confirmed by FTIR studies. TEM results reveal that the size of $CoFe_2O_4$ nanoparticles can be controlled by the addition of SDS. Dielectric study reveals that the dielectric constant increases with increasing SDS concentration. Magnetic studies demonstrate the maximum M_s (138.75 emu/g), H_c (775.69 O_e) and M_r (60.23 emu/g) values for 0.08 M SDS added $CoFe_2O_4$ nanoparticles. The high value of M_s indicates that the prepared magnetic nanoparticles are suitable for high frequency applications.

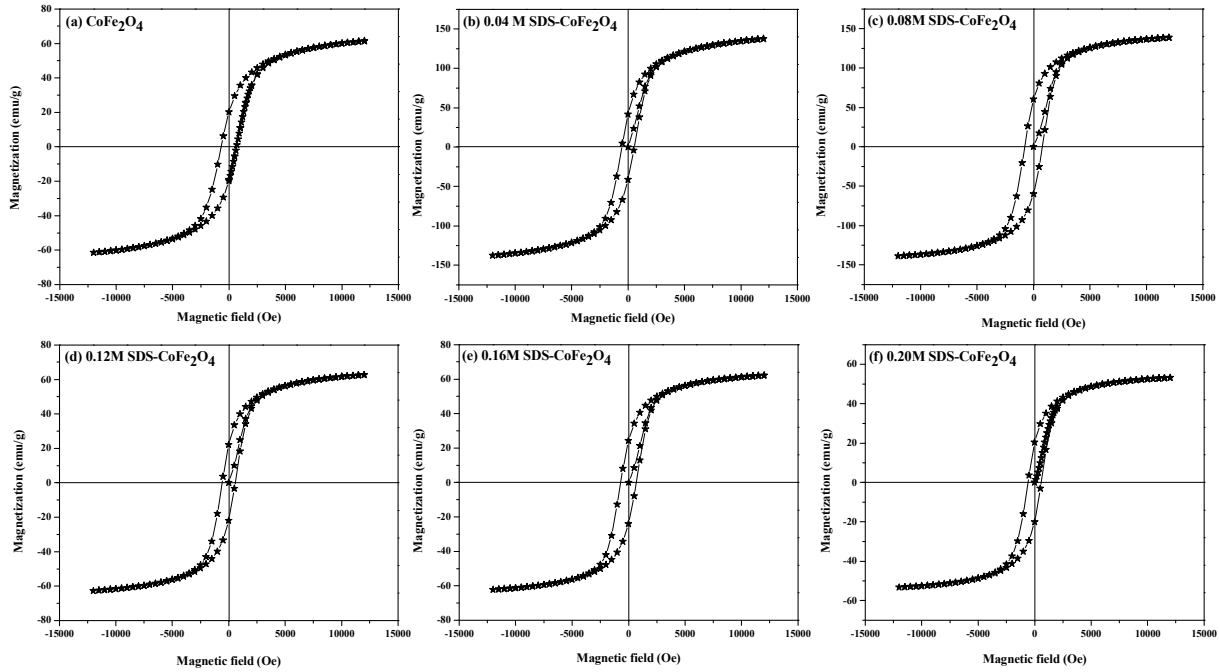

Fig. 9 Room temperature hysteresis loop of (a) $CoFe_2O_4$ and (b) 0.04 M (C) 0.08 M (d) 0.12 M (e) 0.16 M (f) 0.20 M SDS added $CoFe_2O_4$ nanoparticles

Further, the results of the present work reveal that SDS can play an important role in controlling the size of the prepared nanoparticles which in turn influences the magnetic properties of a material.

Acknowledgement

One of the authors M. Vadivel is thankful to UGC-BSR, Government of India for the award of 'Research Fellowship in Science for Meritorious Students-2013'. The authors are thankful to School of Physics, Bharathidasan University, Tiruchirappalli for providing FTIR analysis.

References

1 S.A. Saafan, S.T. Assar, S.F. Mansour, J. Alloys Compd. 542 (2012) 192.
2 M. Bonini, A. Wiedenmann, P. Baglioni, Physica A 339 (2004) 86.
3 He Hu, Zhi-qing Tian, Jie Liang, Hong Yang, An-tao Dai, Lu An, Hui-xia Wu and Shi-ping Yang, Nanotechnology 22 (2011) 085707.
4 P.S. Aghav, V.N. Dhage, M.L. Mane, D.R. Shengule, R.G. Dorik, K.M. Jadhav, Physica B 406 (2011) 4350.
5 R. Nongjai, S. Khan, K. Asokan, H. Ahmed, I. Khan, J. Appl. Phys. 112 (2012) 084321.
6 H.F. Lu, R.Y. Hong, H.Z. Li, J. Alloys Compd. 509 (2011) 10127.
7 S. Ayyappan, S. Mahadevan, P. Chandramohan, M.P. Srinivasan, J. Philip, B. Raj, J. Phys. Chem. C. 114 (2010) 6334.
8 I.H. Gul, A. Maqsood, J. Alloys Compd. 465 (2008) 227.
9 J. Peng, M. Hojamberdiev, Y. Xu, B. Cao, J. Wang, H. Wu, J. Magn. Magn. Mater. 323 (2011) 133.
10 C. Cannas, A. Ardu, D. Peddis, C. Sangregorio, G. Piccaluga, A. Musinu, J. Colloid Interf. Sci. 343 (2010) 415.
11 K. Maaz, S. Karim, A. Mashiatullah, J. Liu, M.D. Hou, Y.M. Sun, J.L. Duan, H.J. Yao, D. Mo, Y.F. Chen, Physica B 404 (2009) 3947.
12 W.A.A. Bayoumy, J. Mol. Struct. 1056–1057 (2014) 285.
13 B. Zhao, B. Hua, H. Wang, Z. Nan, Mater. Lett. 92 (2013) 75.
14 K. Nejati, R. Zabihi, Chem. Cent. J. 6 (2012) 23.
15 P.I.P. Soares, A.M.R. Alves, L.C.J. Pereira, J.T. Coutinho, I.M.M. Ferreira, C.M.M. Novo, J.P.M.R. Borges, J. Colloid Interf. Sci. 419 (2014) 46.
16 L. Shen, Y. Qiao, Y. Guon, S. Meng, G. Yang, M. Wu, J, Zhao, Ceram. Inter. 40 (2014) 1519.
17 D.Y. Chen, Y.Y. Meng, D.C. Zeng, Z.W. Liu, H.Y. Yu, X.C. Zhong, Mater. Lett. 76 (2012) 84.
18 C. Li, Z. Nan, Mater. Lett. 71 (2012) 78.
19 Z. Jing, S. Wu, Mater. Lett. 58 (2004) 3637.
20 Z. Chen, Z. Nan, J. Colloid Interf. Sci. 358 (2011) 416.
21 M. Vadivel, R. Ramesh Babu, K. Sethuraman, K. Ramamurthi, M. Arivanandhan, J. Magn. Magn. Mater. 362 (2014) 122.
22 B.D. Cullity, S.R. Stock, Elements of X-ray Diffraction (3rd ed.) Prentice-Hall, New York (2001).
23 M.A. Gabal, S. Kosa, T.S. Almutairi, J. Magn. Magn. Mater. 356 (2014) 37.
24 A. Baykal, N. Kasapoglu, Y. Koseoglu, M.S. Toprak, H. Bayrakdar, J. Alloys Compd. 464 (2008) 514.
25 G. Dixit, J.P. Singh, R.C. Srivastava, H.M. Agrawal, J. Magn. Magn. Mater. 345 (2013) 65.
26 G.B. Ji, S.L. Tang, S.K. Ren, F.M. Zhang, B.X. Gu, Y.W. Du, J. Cryst. Growth, 270 (2004) 156.
27 A. Thakur, R.R. Singh, P.B. Barman, J. Magn. Magn. Mater. 326 (2013) 35.
28 K. Sultan, M. Ikram, K. Asokan, Vacuum, 99 (2014) 251.